

# Heat Source/Sink and Aligned Magnetic Field effects on Convective flow of a Newtonian fluid past an inclined vertical plate in conducting field.

Sujatha S<sup>1</sup> and Dr.G.S.Prasad<sup>2</sup>

<sup>1</sup>Assistant Professor, Department of Mathematics, The oxford college of Engineering, Bangalore-56008, Karnataka, India.

<sup>2</sup>Professor, Department of Mathematics, AMC college of Engineering, Bangalore -560083, Karnataka, India.

## ABSTRACT:

An analysis is carried out to study the effects of Soret, aligned magnetic field and convective heat and mass transfer flow past an inclined magnetic field over a infinite vertical plate embedded in a porous medium in the presence of the chemical reaction, viscous and joules dissipation. The governing partial differential equations are transformed to non-linear ordinary differential equations by using the regular perturbation technique and then solved numerically by using MATLAB. The effect of various non-dimensional governing parameters on velocity, concentration profiles along skin friction coefficient and rate of mass transfer at the plate are discussed and presented through graphs and tables.

**Keywords:** Heat and Mass transmission, MHD, Permeable object, Inclined Magnetic field, mixed convective flow.

Date of Submission: 13-04-2022

Date of Acceptance: 29-04-2022

## I. INTRODUCTION

The magnetic field analysis in the fluid movement of electrically conducting substances has captured the attention of several scholars, given that there are many diverse areas where it can be used. The industrial use of MHD (magnetic hydrodynamics) is prominent in the oil and gas industry, earth science, space science, and astronomy. Electromagnetic flow field control is a flowfield topic that involves magnetic motions in addition to electrically conducting fluids. In this experiment, magnetic forces are used to bring electrically leading fluids into contact with nonmagnetic fluids, and fluids are studied in connection with electric currents (e.g., plasma, electrolytes, liquid metals, etc.). Gribben [1] studied MHD boundary layer flow across a semi-inclined disc, set up using a magnetic gradient, to see if the structure's varied flow orientation has on either side of the interface. In the laboratory, the flow of a chemically reacting fluid and inspected by PrabaraReddy [2] was analyzed using separate research apparatuses. A dynamic process in which the field had been perturbed by aligning a magnetic dipole [source of flow] in a semi-infinite plate with unidirectional forces is researched by Takhar [3].

Predictable coolants likely H<sub>2</sub>O, ethylene glycols, propylene glycols as well as oils possess small heat conductance this is impediment toward the paths of developing systems heat efficiencies. That is leading to growth of narrative coolants and having highest heat conductance. One of the potential ways to progress heat conductivities of predictable coolants was adding of nano shaped particles in them. It can dissipated most temperature owing to highest heat conductivities ensuing in progressed heat performances of systems. Recurrently utilized nano particles included metals (Copper, Silver, Nickel, Gold), metals oxide (Aluminium trioxide, Copper oxide, Magnesium oxide, Zinc oxide, Silicon dioxide, Ferric trioxide, Titanium dioxide), metals carbides (SiC), metals nitrides (AlN) as well as carbons material (CNTs, MWCNTs, diamonds, graphites). The heat conductance of nano liquid was dependent on plentiful factors they are types, shapes, sizes in addition to stability of dissolved nano particles, types of support liquid utilized, concentrations of nano particles as well as liquid temperatures [4–8].

Natural convection, also known as free convection, is a spontaneous movement caused by non-homogeneous fields with volumetric forces

such as Coriolis, MHD, magnetic, centrifugal, etc. Several scholars have investigated this effect. Free/natural convection flow has a wide variety of functional applications and environmental conditions, including chilling of electronic equipment, geothermal systems, material handling, thermal insulation designs, energy system protection, ambient flows, and air conditioning systems. Furthermore, heat transfer systems, including the movement of material in a flowing fluid medium, have diverse real-world applications. On the planet, specific flows are influenced not only by temperature fluctuations but also by concentration variations. Buoyancy is often essential in atmospheric science, where differences in land and air temperatures can lead to complicated flow shapes. Because of its multiple applications in industry, science, and engineering processes, the analysis of the combined transfer of heat and mass through free convection has piqued the attention of several theoretical models and experimental/practical aspects. In the literature, such questions have been addressed using Newtonian/non-Newtonian fluids for various geometries, including elliptical, rectangular or square, triangle, circular cylinders, and numerical, theoretical, and experimental methods. It is possible to monitor an electrically conducting fluid flow with an external magnetic field restriction. Controlling the transfer rate is often possible. Many sciences and technologies have industrial applications, such as cooling nuclear reactors, boundary layer control in aerodynamics, plasma studies, petroleum industries, crystal development, etc. Consequently, the analysis of the more general circumstances of MHD with the effect of the outward force of the magnetic field on electrically conduction fluid has gained renewed focus from the authors.

Although research and technology continue to pursue different goals in different missions and various fields, specific industrial applications can be

found in some of both, for example, in the study of nuclear reactors, in the boundary layer formation of minerals, and the manipulation of plasmas, such as plasma. The discovery of this broadened the application of MHD and elevated it to the prominence of magnetic fields' effects on electrically conducting fluids. GVN Prasad et al. [9] have discussed Finite Element Analysis of Free Convection Heat Transfer Flow in a Vertical Conical Annular Porous Medium. GVN Prasad et al. [10] have analyzed MHD flow of a Visco-elastic fluid over an unbounded rotating porous plate with Heat source and Chemical reaction.

Although Soret and Fick's effects are more negligible concerning Fourier's and Fick's ideas, the Fourier's and Fick's theories remain common because they explain the large-enough amounts of heat and mass transfer. As with all of the previous expansions, these physical effects are known as secondary phenomena and are likely to be more apparent in hydrology, petrology, etc. It had an order of magnitude value so that it had to be examined by Drake [11]. Soret (thermal diffusion) and Dufour (diffusion thermo) are very important for the fluids with light and medium molecular weight, as stated by many researchers Dursunkaya and Worek [13], Anghel et al. [12]. Rather than being expanded or improved, MHD diffusion-the molecular effects on the convective heat and mass transfer over an inclined surface, Prasad [14] recently researched and tested the impact of diffusive and porous media on the convective heat and mass transfer.

The aim of the research in this article is to describe the temperature. Mass transfer for both plates flows in a porous medium embedded in the nonuniform magnetic field on a convective fluid in the presence of a chemical reaction on the horizontal substrate, with a Heat Soret parameter a magnetic field applied in a stationary source of heat.

## II. PHYSICAL CONFIGURATION AND MATHEMATICAL FORMULATION

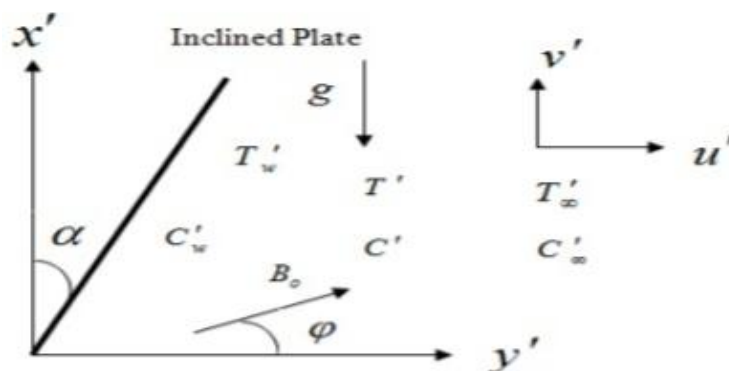


Figure 1: Physical Configuration of the problem

We obtained 2D MHD flow solution and magnetic field line solutions of the problem of free-fluid and charged viscous flow through an angle-porous plate in combination with magnetic and concentration density-induced buoyancy, which are also considered to see how they travel around the plate concerning each other, and then varied the flow fields to see how the resulting magnetic and density fields differ in the relationship. The X-axis is set parallel to the plate's surface, and the Y-axis is positioned parallel to the plate's surface (See Fig.1). Since magnetic Reynolds number is generally

believed to be negligible, it is assumed that Reynolds' number has expanded. It is thought that there is no voltage being applied, which rules out the possibility of an electrical field. This misunderstanding about Joule's equation leads to many thinking that the halls, electrical effects, and polarisation effects being ignored in the energy equation led to the belief that dissipation had been overlooked. As the assumptions above are postulated, those governing are satisfied, the following must also be faithful:

$$\frac{\partial v^*}{\partial y^*} = 0 \rightarrow v^* = -v_0 (v_0 > 0) \quad (1)$$

$$v^* \frac{\partial u^*}{\partial y^*} = g \frac{\partial^2 u^*}{\partial y^{*2}} + g\beta(T^* - T_\infty) \cos \alpha + gB^*(C^* - C_\infty) \cos \alpha - \frac{\sigma B_0^2}{\rho} \sin^2 \gamma u^* - \frac{g u^*}{k^*} \quad (2)$$

$$v^* \frac{\partial T^*}{\partial y^*} = \frac{k}{\rho C_p} \frac{\partial^2 T^*}{\partial y^{*2}} + \frac{g}{C_p} \left( \frac{\partial u^*}{\partial y^*} \right)^2 + \frac{\sigma B_0^2}{\rho} u^{*2} + \frac{Q_0}{\rho C_p} (T^* - T_\infty) \quad (3)$$

$$v^* \frac{\partial C^*}{\partial y^*} = D \frac{\partial^2 C^*}{\partial y^{*2}} + D_1 \frac{\partial^2 T^*}{\partial y^{*2}} - K_1 (C^* - C_\infty) \quad (4)$$

The frontier stipulations for the given problems were specified for the velocity, temperature and concentration fields are

$$u^* = 0 \quad T^* = T_w, \quad C^* = C_w \quad \text{at } y^* = 0$$

$$u^* \rightarrow 0, \quad T^* \rightarrow T_\infty, \quad C^* \rightarrow C_\infty \quad \text{as } y^* \rightarrow \infty \quad (5)$$

More explicitly, one can write down the field equations (2) to (4) in the form of non-dimensionality.

$$u = \frac{u^*}{v_0}, \quad y = \frac{v_0 y^*}{g}, \quad \text{Pr} = \frac{g \rho C_p}{k}, \quad \theta = \frac{T^* - T_\infty}{T_w - T_\infty}, \quad \varphi = \frac{C^* - C_\infty}{C_w - C_\infty}, \quad Gr = \frac{g \beta (T_w - T_\infty)}{v_0^3}$$

$$Gm = \frac{g \beta_c (C_w - C_\infty)}{v_0^3}, \quad Ec = \frac{v_0^2}{C_p (T_w - T_\infty)}, \quad M^2 = \frac{\sigma B_0^2 g}{\rho v_0^2}, \quad k^* = \frac{g^2}{K_0 v_0^2}, \quad g = \frac{\mu}{\rho}, \quad S_c = \frac{g}{D} \quad (6)$$

$$S_0 = \frac{D_1 (T_w - T_\infty)}{g (C_w - C_\infty)}, \quad Kr = \frac{g K_1}{v_0^2}, \quad Q = \frac{Q_0 g}{\rho C_p v_0^2}$$

The basic field equations (2) – (4), can be expressed in non- dimensional form as

$$\frac{\partial u^2}{\partial y^2} + \frac{\partial u}{\partial y} - (M^2 \sin^2 \gamma - K_0) u = -G_r \cos \alpha \theta - G_m \cos \alpha \varphi \quad (7)$$

$$\frac{\partial^2 \theta}{\partial y^2} + \text{Pr} \frac{\partial \theta}{\partial t} + \text{Pr} E_c \left( \frac{\partial u}{\partial y} \right)^2 + \text{Pr} Ec M^2 u^2 + \text{Pr} Q \theta = 0 \quad (8)$$

$$\frac{\partial^2 \varphi}{\partial y^2} + S_c \frac{\partial \varphi}{\partial t} - S_c Kr \varphi + S_0 S_c \frac{\partial^2 \theta}{\partial y^2} = 0 \quad (9)$$

The frontier stipulations for the given problems were specified in dimensionless form

$$\text{At } y^* = 0, \quad u = 0, \quad \theta = 1, \quad \varphi = 1$$

$$\text{As } y^* \rightarrow \infty, u \rightarrow 0, \theta \rightarrow 1, \phi \rightarrow 1 \tag{10}$$

To solve the equations (7) - (9) with relevant boundary conditions (10) with the flowing Eqns. for the velocity, temperatures  $\ll \epsilon$  with the help of perturbation technique as well as concentrations distributions were presumed as

$$u(y, t) = u_0(y) + E_c u_1(y) + O(Ec^2)$$

$$\theta(y, t) = \theta_0(y) + E_c \theta_1(y) + O(Ec^2)$$

$$\phi(y, t) = \phi_0(y) + E_c \phi_1(y) + O(Ec^2)$$

(11)

Equation (11) of expressions in (7)–(9) the coefficient of like powers of Ec is found to be, as per Equation 7-9.

Zero order terms:

$$u_0'' + u_0' - (M^2 \sin^2 \gamma + K_0) u_0 = -Gr \cos \alpha \theta_0 - Gm \cos \alpha \phi_0 \tag{12}$$

$$\theta_0'' + Pr \theta_0' - Pr Q \theta_0 = 0 \tag{13}$$

$$\phi_0'' + Sc \phi_0' - Sc Kr \phi_0 = -S_c S_0 \theta_0'' \tag{14}$$

First order terms:

$$u_1'' + u_1' - (M^2 \sin^2 \gamma + K_0) u_1 = -Gr \cos \alpha \theta_1 - Gm \cos \alpha \phi_1 \tag{15}$$

$$\theta_1'' + Pr \theta_1' + Pr Q \theta_1 = -Pr (u_0')^2 - Pr M^2 u_0^2 \tag{16}$$

$$\phi_1'' + Sc \phi_1' - Sc Kr \phi_1 = -Sc S_0 \theta_1'' \tag{17}$$

In order to fulfill the corresponding boundary conditions, proceed as follows:

$$u_0 = 0, u_1 = 0, \theta_0 = 1, \theta_1 = 0, \phi_0 = 1, \phi_1 = 0 \quad \text{at } y = 0$$

$$u_0 \rightarrow 0, u_1 \rightarrow 0, \theta_0 \rightarrow 0, \theta_1 \rightarrow 0, \phi_0 \rightarrow 0, \phi_1 \rightarrow 0 \quad \text{as } y \rightarrow \infty$$

(18)

under the boundary conditions (18), with expanding equations (12) - (17) we obtained

$$\theta_0 = \exp(-l_1 y)$$

(19)

$$\phi_0 = b_1 \exp(-l_1 y) + b_2 \exp(-l_2 y) \tag{20}$$

$$u_0 = b_3 \exp(-l_1 y) + b_4 \exp(-l_2 y) + b_5 \exp(-l_3 y) \tag{21}$$

$$\theta_1 = b_6 \exp(-2l_1 y) + b_7 \exp(-2l_2 y) + b_8 \exp(-2l_3 y) + b_9 \exp(-(l_1 + l_2) y) + b_{10} \exp(-(l_3 + l_2) y) + b_{11} \exp(-(l_1 + l_3) y) + b_{12} \exp(-l_4 y)$$

(22)

$$\phi_1 = b_{13} \exp(-l_4 y) + b_{14} \exp(-2l_1 y) + b_{15} \exp(-2l_2 y) + b_{16} \exp(-2l_3 y) + b_{17} \exp(-(l_1 + l_2) y) + b_{18} \exp(-(l_3 + l_2) y) + b_{19} \exp(-(l_1 + l_3) y) + b_{20} \exp(-l_5 y) \tag{23}$$

$$u_1 = b_{21} \exp(-l_4 y) + b_{22} \exp(-2l_1 y) + b_{23} \exp(-2l_2 y) + b_{24} \exp(-2l_3 y) + b_{25} \exp(-(l_1 + l_2) y) + b_{26} \exp(-(l_3 + l_2) y) + b_{27} \exp(-(l_1 + l_3) y) + b_{28} \exp(-l_5 y) + b_{29} \exp(-l_6 y)$$

(24)

On solving Eqns. (19) – (24) making utilize of the frontier conditions (18), it was obtained as,

$$u(y, t) = b_3 \exp(-l_1 y) + b_4 \exp(-l_2 y) + b_5 \exp(-l_3 y) + E_c [b_{21} \exp(-l_4 y) + b_{22} \exp(-2l_1 y) + b_{23} \exp(-2l_2 y) + b_{24} \exp(-2l_3 y) + b_{25} \exp(-(l_1 + l_2) y) + b_{26} \exp(-(l_3 + l_2) y) + b_{27} \exp(-(l_1 + l_3) y) + b_{28} \exp(-l_5 y) + b_{29} \exp(-l_6 y)] \tag{25}$$

$$\theta(y, t) = \exp(-l_1 y) + E_c [b_6 \exp(-2l_1 y) + b_7 \exp(-2l_2 y) + b_8 \exp(-2l_3 y) + b_9 \exp(-(l_1 + l_2) y) + b_{10} \exp(-(l_3 + l_2) y) + b_{11} \exp(-(l_1 + l_3) y) + b_{12} \exp(-l_4 y)] \quad (26)$$

$$\phi(y, t) = b_1 \exp(-l_1 y) + b_2 \exp(-l_2 y) + E_c [b_{13} \exp(-l_4 y) + b_{14} \exp(-2l_1 y) + b_{15} \exp(-2l_2 y) + b_{16} \exp(-2l_3 y) + b_{17} \exp(-(l_1 + l_2) y) + b_{18} \exp(-(l_3 + l_2) y) + b_{19} \exp(-(l_1 + l_3) y) + b_{20} \exp(-l_5 y)] \quad (27)$$

**Skin Friction:**

In favour of engineering attention, it was determined the skin frictions, Nusselts quantity as well as Sherwoods quantity near the plate. The shearing stresses near the plate as well as it was given by,

$$\begin{aligned} \tau &= \left( \frac{\partial u}{\partial y} \right)_{y=0} \\ &= \left( \frac{\partial u_0}{\partial y} \right)_{y=0} + E_c \left( \frac{\partial u_1}{\partial y} \right)_{y=0} \\ \tau &= -(b_3 l_1 + b_4 l_2 + b_5 l_3) - E_c [b_{21} l_4 + 2 b_{22} l_1 y + 2 b_{23} l_2 + 2 b_{24} l_3 + b_{25} (l_1 + l_2) + b_{26} (l_3 + l_2) + b_{27} (l_1 + l_3) + b_{28} l_5 + b_{29} l_6 y] \end{aligned} \quad (28)$$

**Nusselt Number :**

The rates of temperature transportation near the plate (Nusselts quantity) was given through,  $N_u = \left( \frac{\partial \theta}{\partial y} \right)_{y=0}$

$$\begin{aligned} &= \left( \frac{\partial \theta_0}{\partial y} \right)_{y=0} + E_c \left( \frac{\partial \theta_1}{\partial y} \right)_{y=0} \\ &= -l_1 - E_c [2 b_6 l_1 + 2 b_7 l_2 + 2 b_8 l_3 + b_9 (l_1 + l_2) + b_{10} (l_3 + l_2) + b_{11} (l_1 + l_3) + b_{12} l_4] \end{aligned} \quad (29)$$

**Sherwood Number :**

The rates of mass transportation near the plate (Sherwoods quantity) was given by

$$\begin{aligned} Sh &= \left( \frac{\partial \phi}{\partial y} \right)_{y=0} \\ &= \left( \frac{\partial \phi_0}{\partial y} \right)_{y=0} + \left( \frac{\partial \phi_1}{\partial y} \right)_{y=0} \\ &= -(b_1 l_1 + b_2 l_2) - E_c [b_{13} l_4 + 2 b_{14} l_1 + 2 b_{15} l_2 + 2 b_{16} l_3 + b_{17} (l_1 + l_2) + b_{18} (l_3 + l_2) + b_{19} (l_1 + l_3) + b_{20} l_5] \end{aligned} \quad (30)$$

**III. RESULTS AND DISCUSSION**

The Heat source as well as Aligned magnetic field effects on the MHD liberated convection revolving flows of a semi unlimited porous stirring plate with the invariable temperature resource was considered. Making utilize of the perturbations methodology, it was found velocity, temperatures as well as concentrations distributions. In ordered to fetch out the significant characteristics of the flow domain, heat as well as mass transportation characteristics with nano particles, the results were displayed by the Figs.2–16 as well as in Tables. 1–3. The effects by flow parameters on

velocity, temperatures as well as concentrations Heat source and Aligned magnetic field, the skin frictions, the rates of temperatures as well as mass transportation coefficients have been explored computationally.

**Velocity Profiles:**

Expression 2 indicates the impact of an inclined angle  $\alpha$  on the velocity profile. Figure 2: First, the velocity is gradually lessened with increasing values of the inclination, as shown by the slope of the initial and final velocity vs the corresponding angle, second-order tangent values. If

the magnetic field strength is set to Aligned magnetic field  $\gamma$ , Figure 3 depicts the influence of field strength on velocity. We found that the speed goes down the farther you go from the magnetic field, the faster the object is moving. The figures in figure 4 demonstrate the significance of the influence of the thermal Grashof amount, or scale factor, on velocity. This graph reveals that fluid velocity rises with the order-of-of-of-magnitude rise values. Because of the buoyancy, the water pushes up on the bodies during acceleration, thereby increasing the velocity. This is shown in Figure 5, where the results of the magnetic parameter  $M$  are plotted on the  $y$ - as the input of these cases' produces increasingly smaller and smaller results as they get through this statistic, we find that the result is also decreasing. This is attributable to transverse magnetic power, regarded as the Lorentz force. Figure 6 shows the profiles of the velocity for spans along the coordinate  $z$  and permeability on the

vertical scales in the presence of scaling. With decreasing permeability constant  $Ko$ , we find the velocity diminishes. It is compared to a collection of figures in Figure 7 concerning the changed Grashof numbers. We will see that modified Grashof velocity is higher when the modified Grashof-amount rises, even in terms of the velocity profiles' influence on various values of the chemical reaction. We can relate to those in the drawing  $(Kr)$ . As Schmidt's number grows, the velocity of the blue curve decreases as it does in figure 9. The Soret temperature on the light strength of a visual picture is different, based on whether the Expand setting is maximum or minimum. A simple way to think about it is by comparing parametric images of a line with other continuous-function plots to Soret's images. From the diagrams, it indicates that in Figure 11, the reversal activity takes place for increasing the Prandtl number

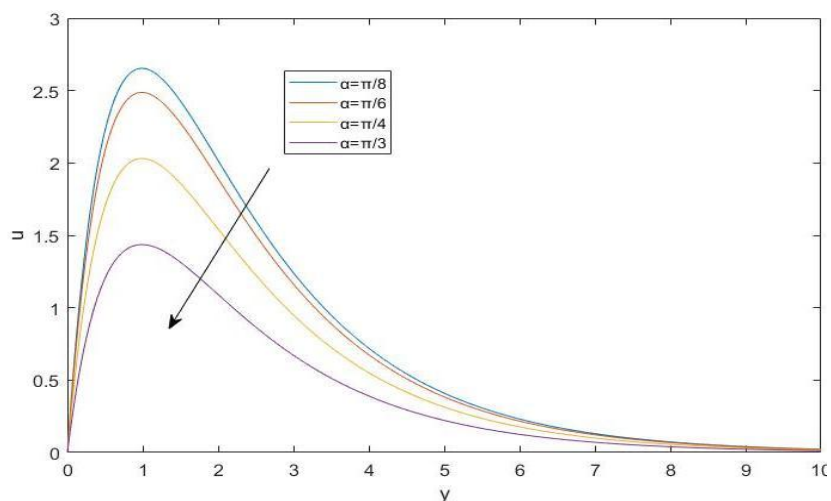


Fig 2: variations of velocity values of  $\alpha$ .  $So=0.5$ ,  $\gamma = \pi/6$ ,  $Sc=0.6$ ,  $Pr=0.71$ ,  $Gr=5$ ,  $Ko=1$ ,  $Kr=0.1$ ,  $M=1$ ,  $Q=0.1$ ,  $R=1$ ,  $Gm=5$ ,  $Ec=0.001$

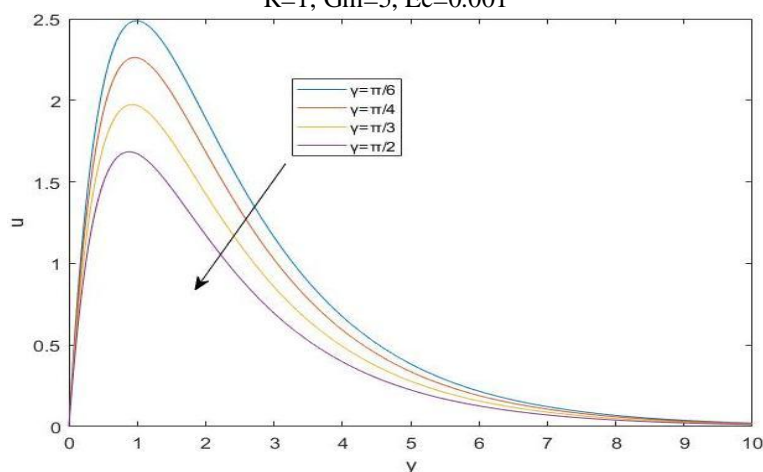


Fig 3: variations of velocity values of  $\alpha$ .  $So=0.5$ ,  $\alpha = \pi/6$ ,  $Sc=0.6$ ,  $Pr=0.71$ ,  $Gr=5$ ,  $Ko=1$ ,  $Kr=0.1$ ,  $M=1$ ,  $Q=0.1$ ,  $R=1$ ,  $Gm=5$ ,  $Ec=0.001$

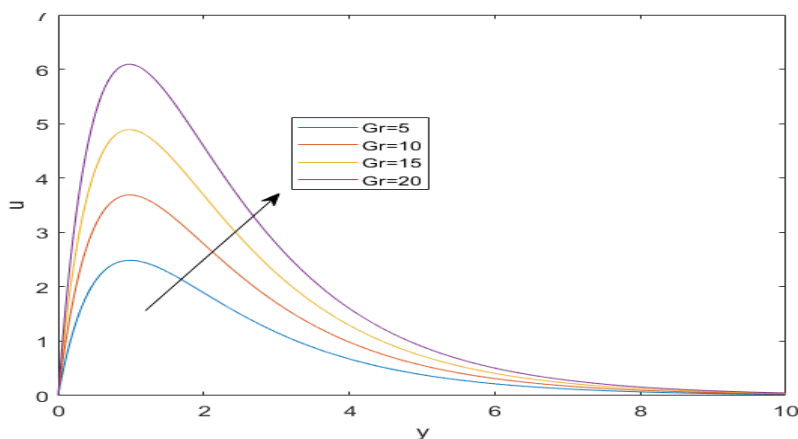


Fig 4: variations of velocity values of Gr. So=0.5, Sc=0.6, Pr=0.71, Ko=1,  $\gamma=30$ ,  $\alpha=30$ , Kr=0.1, M=1, Q=0.1, R=1, Gm=5, Ec=0.001

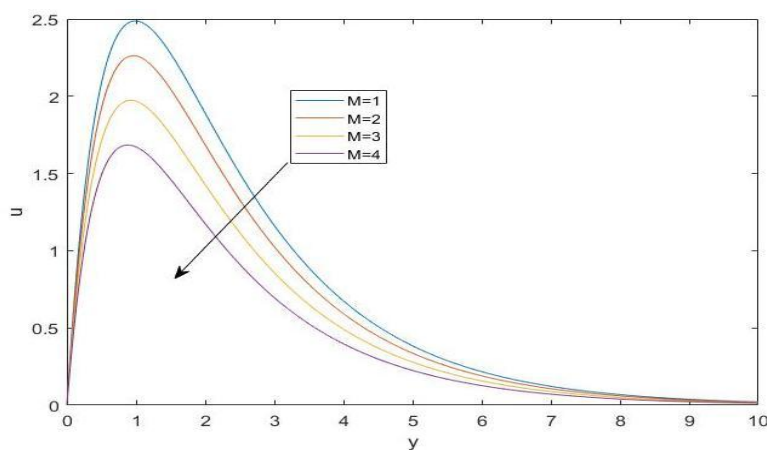


Fig 5: variations of velocity values of M. So=0.5, Sc=0.6, Pr=0.71, Ko=1,  $\gamma=30$ ,  $\alpha=30$ , Kr=0.1, Gr=5, Q=0.1, R=1, Gm=5, Ec=0.001

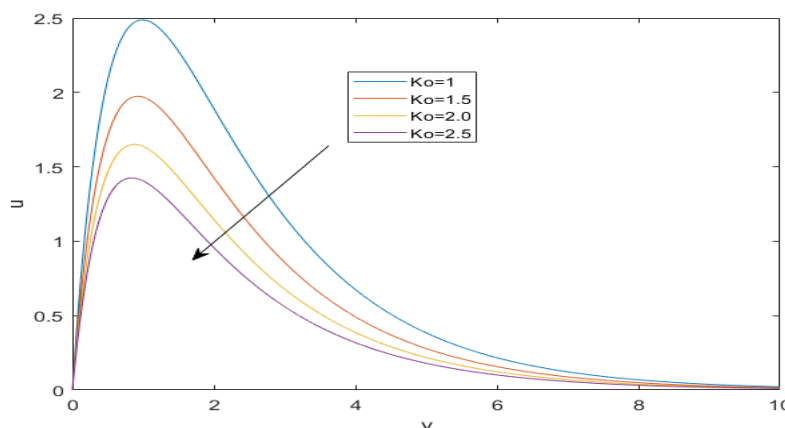


Fig 6: variations of velocity values of Ko. So=0.5, M=1, Sc=0.6, Pr=0.71,  $\alpha=30$ , Kr=0.1,  $\gamma=30$ , Gr=5, Q=0.1, R=1, Gm=5, Ec=0.001

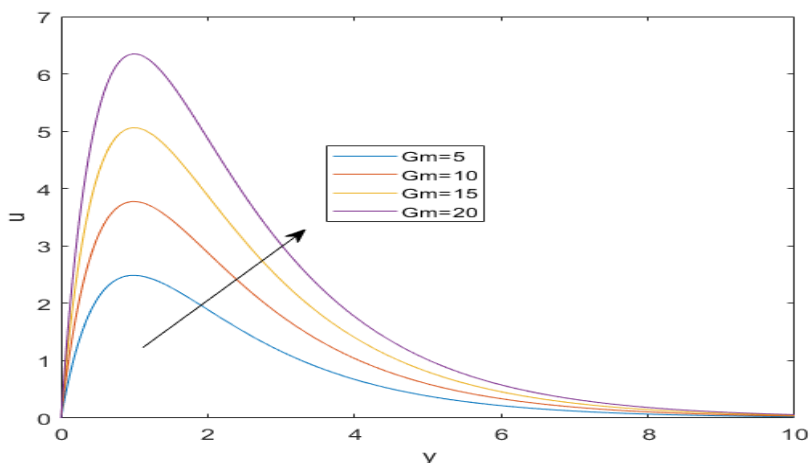


Fig 7: variations of velocity values of  $Gm$ .  $So=0.5, M=1, Sc=0.6, Pr=0.71, Ko=1, \alpha=30, \gamma=30, Kr=0.1, Gr=5, Q=0.1, R=1, Ec=0.001$

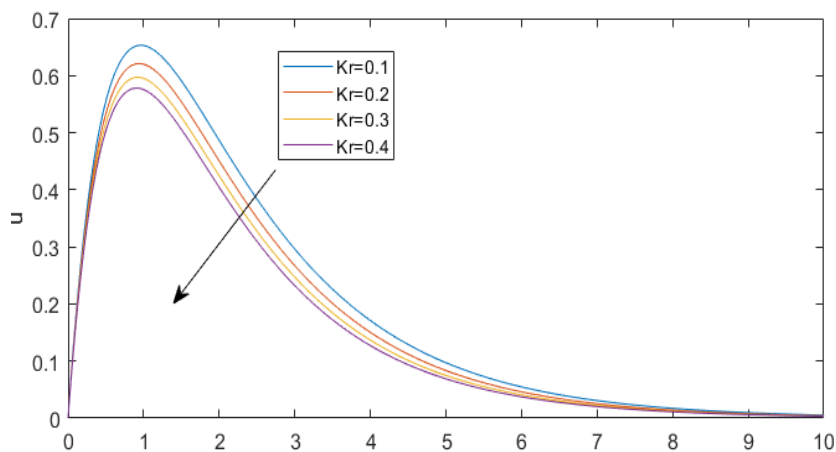


Fig 8: variations of velocity values of  $Kr$ .  $So=0.5, M=1, Sc=0.6, Pr=0.71, Ko=1, \alpha=30, \gamma=30, Gr=5, Q=0.1, R=1, Gm=5, Ec=0.001$

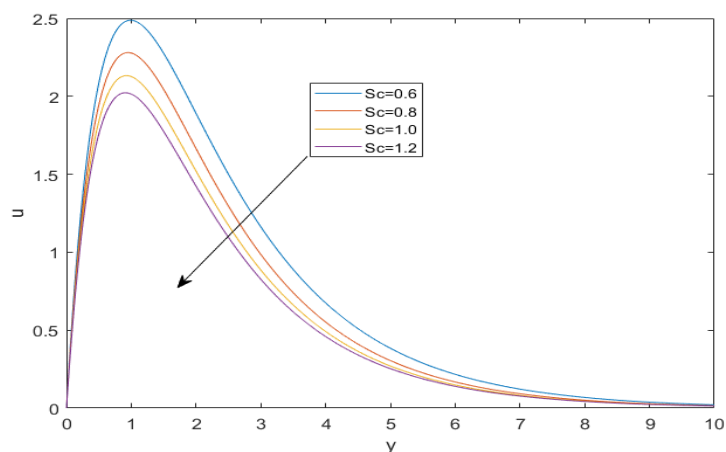


Fig 9: variations of velocity values of  $Sc$ .  $So=0.5, M=1, Pr=0.71, Ko=1, \alpha=30, \gamma=30, Kr=0.1, Gr=5, Q=0.1, R=1, Gm=5, Ec=0.001$

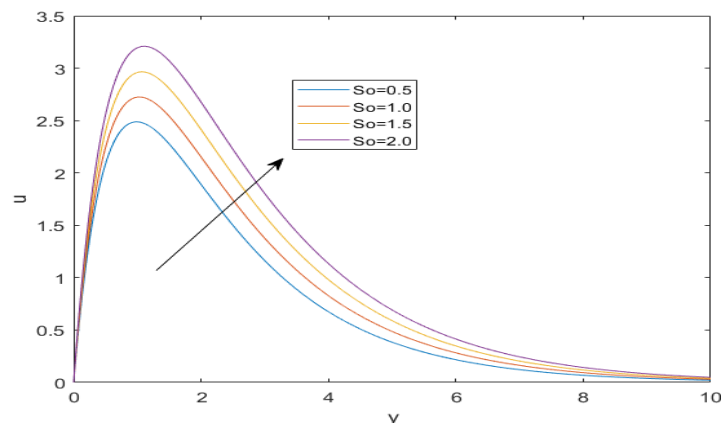


Fig 10: variations of velocity values of  $So$ .  $M=1, Sc=0.6, Pr=0.71, Ko=1, \alpha=30, \gamma=30, Kr=0.1, Gr=5, Q=0.1, R=1, Gm=5, Ec=0.001$

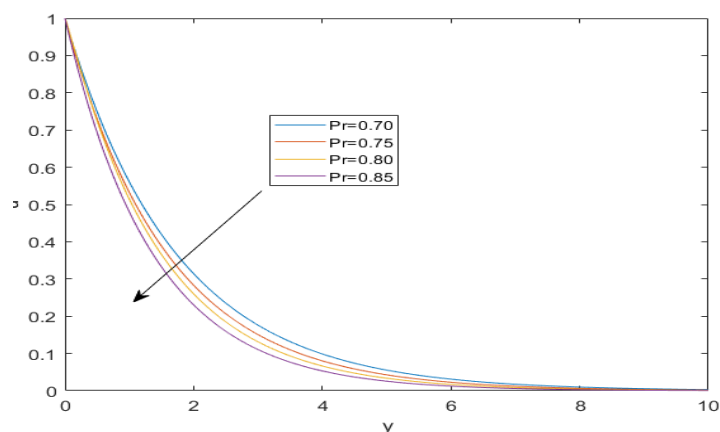


Fig 11: variations of velocity values of  $Pr$ .  $So=0.5, M=1, Sc=0.6, Pr=0.71, Ko=1, \alpha=30, \gamma=30, Kr=0.1, Gr=5, Q=0.1, R=1, Gm=5, Ec=0.001$

**Temperature Profiles:**

Figure 12 shows the results of the effect of heat source  $Q$  on the temperature distribution. the thermometer can react to an increasing heat parameter, or source, as compared to a rise in the  $Q$ . Figure 13 presents the numerous temperature

profiles if you're interested in learning about Prandtl's number. If the Prandtl number goes up, the temperature falls; it is found that the drop in temperature becomes less critical. As the Prandtl number decreases, so does the thermal conductivity, and so does the surface heat diffusion.

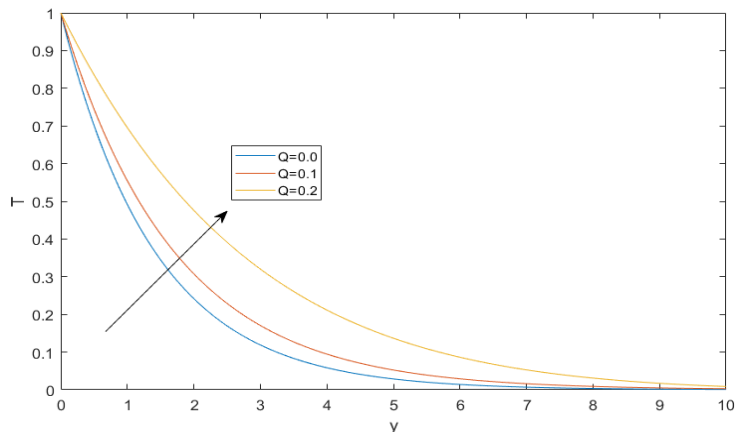


Fig 12. Consistency-temperature profiles with various values of  $Q$ .  $So=0.5, M=1, Sc=0.6, Pr=0.71, Ko=1, \alpha=30, \gamma=30, Kr=0.1, Gr=5, R=1, Gm=5, Ec=0.001$

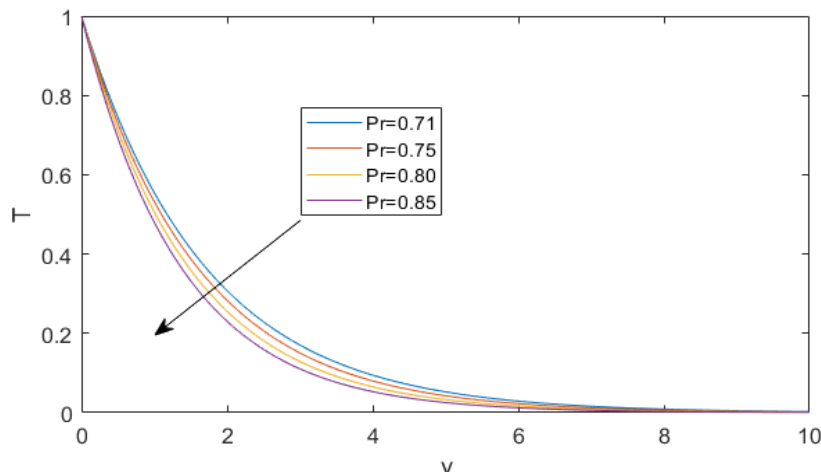


Fig 13: Consistency-temperature profiles with various values of Pr. So=0.5, M=1, Sc=0.6, Q=0.1, Ko=1,  $\alpha=30$ ,  $\gamma=30$ , Kr=0.1, Gr=5, R=1, Gm=5, Ec=0.001

**Concentration Profiles:**

Chemical reaction parameter Kr, Schmidt number sc, and Soret number effect are shown in Figures 14, 15 and 16. As a result, the concentration of species is viewed. The concentration profiles for different values of the chemical reaction Kr are shown in Figure 14. It can be shown in this graph that the concentration rises as the chemical reaction parameter Kr rises. Figure 15 depicts species

concentration profiles for various Schmidt number Sc values. It's evident that as Sc increases, the concentration boundary layer thickness decreases. It's also worth noting that concentration decreases exponentially and eventually reaches the free stream condition for Sc's large values. Finally, we can see in Figure 16 that the concentration rises as the soret parameter is increased.

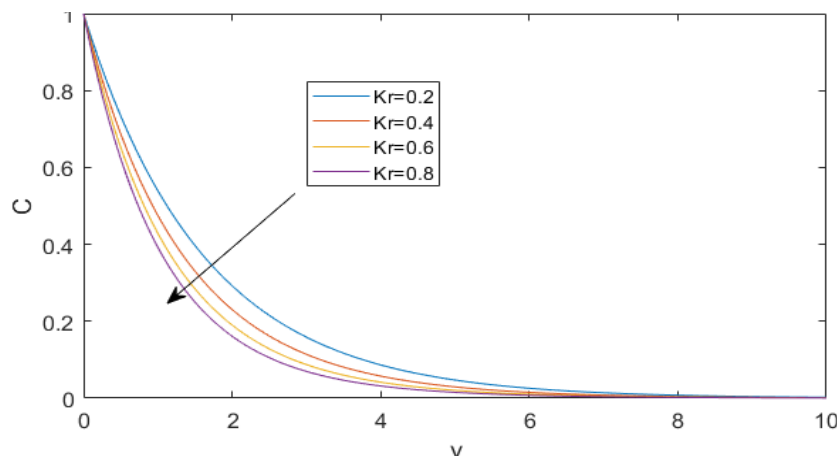


Fig 14: Concentration profiles for different values of Kr.

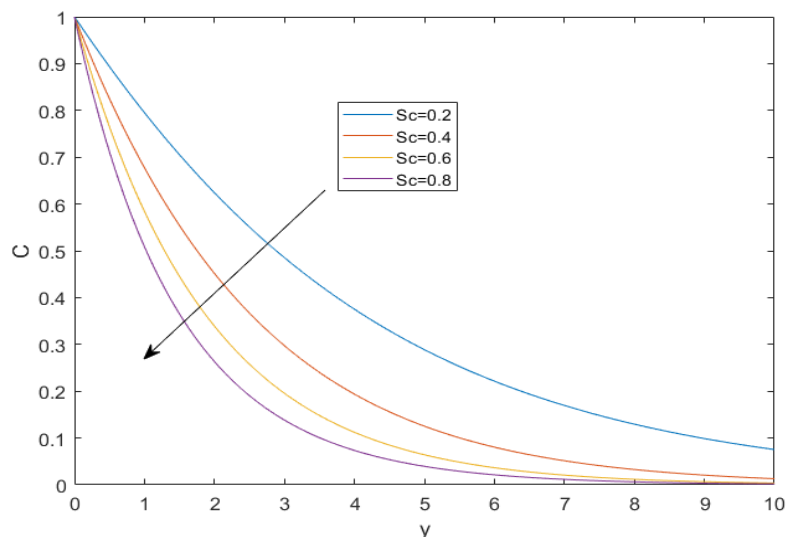


Fig 15: Concentration profiles for different values of  $Sc$

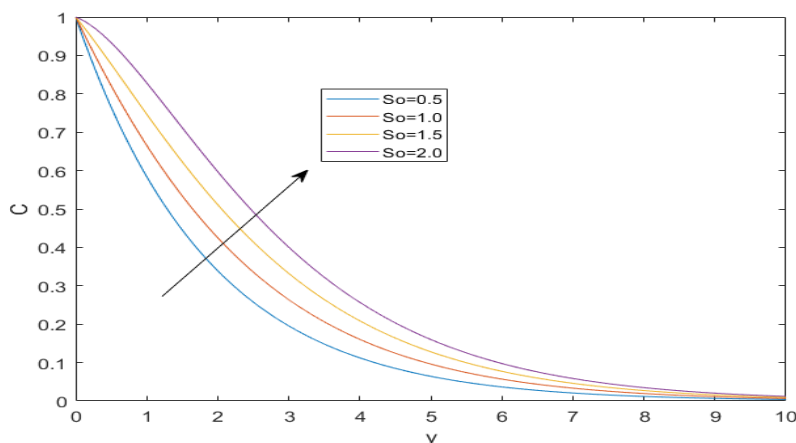


Fig 16: Concentration profiles for different values of  $So$

**Table 1**, demonstrates that the skin-friction quantity enhances with an enhancing in Grashof number ( $Gr$ ), modified Grashof number ( $Gc$ ), Porosity parameter ( $K$ ) and Aligned magnetic field parameter ( $\gamma$ ), where as it diminishes under the influence of magnetic parameter and inclined angle.

**Skin Friction ( $\tau$ )**

| $Gr$ | $Gm$ | $M$ | $Ko$ | $\gamma$ | $\alpha$ | $T$     |
|------|------|-----|------|----------|----------|---------|
| 5    |      |     |      |          |          | 7.1611  |
| 10   |      |     |      |          |          | 10.6733 |
| 15   |      |     |      |          |          | 14.1925 |
|      | 5    |     |      |          |          | 7.1611  |
|      | 10   |     |      |          |          | 10.8155 |
|      | 15   |     |      |          |          | 14.4673 |
|      |      | 1.5 |      |          |          | 6.9677  |
|      |      | 2   |      |          |          | 6.4417  |
|      |      | 2.5 |      |          |          | 5.8393  |
|      |      |     | 1    |          |          | 7.1611  |
|      |      |     | 5    |          |          | 3.6578  |
|      |      |     | 7.5  |          |          | 0.3186  |
|      |      |     |      | $\pi/10$ |          | 0.3187  |
|      |      |     |      | $\pi/6$  |          | 0.3186  |
|      |      |     |      | $\pi/3$  |          | 0.3185  |

|  |  |  |  |  |          |        |
|--|--|--|--|--|----------|--------|
|  |  |  |  |  | $\pi/10$ | 0.3499 |
|  |  |  |  |  | $\pi/6$  | 0.3186 |
|  |  |  |  |  | $\pi/3$  | 0.1840 |

**Table 2,** demonstrates that the Nusselt quantity enhances with an enhancing Eckert Number where as it diminishes under the influence of Prandtl and Heat absorption specifications.

**Nusselt Number (Nu)**

| Pr   | Ec | Q    | Nu      |
|------|----|------|---------|
| 0.75 |    |      | -0.6312 |
| 0.80 |    |      | -0.6828 |
| 0.85 |    |      | -0.7342 |
|      | 1  |      | -0.5879 |
|      | 5  |      | -0.5810 |
|      | 10 |      | -0.5724 |
|      |    | 0.1  | -0.4717 |
|      |    | 0.15 | -0.5144 |
|      |    | 0.20 | -0.5366 |

**Table 3,** demonstrates the quantity of Sherwood expanding with enhancing numerous of Soret and where as diminishes with enhancing the values of Schmidt and the Chemical reaction specifications.

**Sherwood Number (Sh)**

| Sc  | So  | Kr    | Sh      |
|-----|-----|-------|---------|
| 0.6 |     |       | -0.6145 |
| 1.2 |     |       | -1.1013 |
| 1.8 |     |       | -2.5014 |
|     | 0.5 |       | -0.6145 |
|     | 1.0 |       | -0.4529 |
|     | 1.5 |       | -0.2608 |
|     |     | 0.001 | 0.3581  |
|     |     | 0.003 | 0.1430  |
|     |     | 0.005 | 0.0052  |

#### IV. CONCLUSION

The Heat source as well as Aligned magnetic field effects on the MHD liberated convection revolving flows of a semi unlimited porous stirring plate with the invariable temperature resource was considered. Making utilize of the perturbations methodology, it was found velocity, temperatures as well as concentrations distributions. The findings of this study are as follows.

1. Velocity diminishes for enhancing numerous of the angle of inclination  $\alpha$ , Aligned magnetic field specification  $\gamma$ , magnetic specification M, chemical reaction specification Kr, permeability specification Ko, and Schmidt specification Sc, the reversal behavior is observed in the case of Grashof 'Gr', modified Grashof 'Gm' and Soret 'So' specifications.
2. Temperature distribution decreases with an increase in Prandtl number Pr where as it enhances with increasing heat Source specification Q.
3. Concentration boundary layer diminishes with an enhancing Chemical reaction 'Kr' and

Schmidt 'Sc' where as it is enhances with rising values of Soret 'So' specifications.

4. skin-friction increases with an increase in (Gr), (Gc),(Ko) and ( $\gamma$ ), where as it decreases under the influence of (M) and ( $\alpha$ ).
5. The Nusselts quantity reduces by an increasing Ec and the reversal behavior is observed in Pr and Q.
6. The Sherwood quantity enhances with an increasing in (So),but a reverse effect is noticed in the case of Sc and Kr.

#### REFERENCES

- [1]. R.J. Gribben, "The Magneto hydrodynamic boundary layer in the presence of pressure gradient". Proc.Royal.Soc.london.1965.Vol. A287, pp. 123-141.
- [2]. V.Prabhakara Reddy, R.V.M.S.S.Kiran Kumar, G. Viswanatha Reddy, P. Durga Prasad, and S.V.K. Varma. "Free Convection Heat and Mass Transfer Flow of Chemically Reactive and Radiation Absorption Fluid in

- an Aligned Magnetic Field”. Procedia Engineering. 2015.Vol. 127, pp.575–582.
- [3]. H.S. Takhar, A.J. Chamkha, and G. Nath. “Unsteady Flow and Heat Transfer on a Semi infinite Flat Plate with an Aligned Magnetic Field”. International Journal of Engineering Science, 1999.Vol.37, pp.1723-173.
- [4]. K Raghunath, M Obulesu, Dr R sivaprasad Heat and mass transfer on Unsteady MHD flow of through porous medium between two vertical porous plates, AIP Conference Proceedings 2220, 130003-1-130003-6 (2020); <https://doi.org/10.1063/5.0001103>
- [5]. K. Raghunath, Dr. R.SivaPrasad, & Dr. G.S.S. Raju., Heat and mass transfer on MHD flow of Non-Newtonian fluid over an infinite vertical porous plate” Published in, International Journal of Applied Engineering Research, Volume 13, Number 13 (2018) pp.11156-11163.
- [6]. K. Raghunath, Dr. R.Sivaprasad, & Dr. G.S.S. Raju., “Hall Effects on MHD Convective Rotating Flow of Through a Porous Medium past Infinite Vertical Plate” Published in Annals of Pure and Applied Mathematics, Vol. 16, No. 2, 2018, 353-263,2018, DOI<http://dx.doi.org/10.22457/apam.v16n2a12>.
- [7]. K. Raghunath, Dr. R.Siva Prasad, & Dr. G.S.S. Raju., “Heat and Mass Transfer on Unsteady MHD Flow of a Second grade Fluid Through Porous Medium Between Two Vertical Plates”, Journal of Ultra Scientist of Physical Science”, Volume 30(2), 1-11,(2018).
- [8]. K. Raghunath, Dr. R.Siva Prasad, & Dr. G.S.S. Raju., “Heat and Mass Transfer on Unsteady MHD Flow of a Visco-Elastic Fluid Past an Infinite Vertical Oscillating Porous Plate”, Published in British journal of Mathematics & Computer Science, volume 17(6), 2016, DOI:10.9734/BJMCS/2016/25872.
- [9]. G. Suresh Babu , G. Nagesh , K. Raghunath , Dr. R. Siva Prasad “Finite Element Analysis of Free Convection Heat Transfer Flow in a Vertical Conical Annular Porous Medium” Published in International Journal of Applied Engineering Research, Volume 14, Number 1 (2019) pp. 262-277.
- [10]. G.V Nagendraprasad , G. Nagesh , K. Raghunath , Dr. R. Siva Prasad “MHD flow of a Visco-elastic fluid over an unbounded rotating porous plate with Heat source and Chemical reaction” Published in International Journal of Applied Engineering Research, Volume 13, Number 24 (2019) pp.16927-16938.
- [11]. E.R.G.Eckert, R.M.Drake, “Analysis of Heat and Mass Transfer”. M.C.Graw-Hill, New York, 1972.
- [12]. M.Anghel, H.S Takhar, I.Pop, “Dufour and Soret effects on free convection boundary layer over a vertical surface embedded in a porous medium”. Studia Universitatis Babes-Bolyai, Cluj-Napoca, 2000, Vol.4,pp.11-21.
- [13]. Z. Dursunkaya, W.M.Worek. “Diffusion–thermo and thermal-diffusion effects in transient and steady natural convection from vertical surface”. Int. J. Heat Mass Transf. 1992.Vol. 35, pp.2060-2065.
- [14]. P. Durga Prasad, R.V.M.S.S Kiran Kumar, B.Mamatha, S.V.K. Varma. “Diffusion-thermo and porous medium effects on MHD free convection heat and mass transfer flow over an inclined surface”, Global Journal of Pure and Applied Mathematics. 2016. Vol 12. pp. 142-150.